

Photodissociation dynamics of the reaction $\text{CF}_2\text{Br}_2 + h\nu \rightarrow \text{CF}_2 + 2\text{Br}$. Energetics, threshold and nascent CF_2 energy distributions for $\lambda = 223\text{--}260\text{ nm}$

Melanie R. Cameron,[†] Stephen A. Johns, Gregory F. Metha[‡] and Scott H. Kable*

School of Chemistry, University of Sydney, NSW 2006, Australia.

E-mail: s.kable@chem.usyd.edu.au

Received 11th January 2000, Accepted 3rd April 2000

Published on the Web 12th May 2000

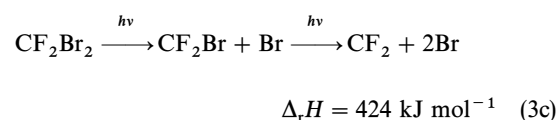
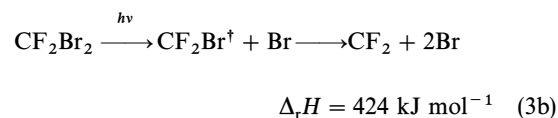
The dissociation dynamics of the reaction $\text{CF}_2\text{Br}_2 + h\nu \rightarrow \text{CF}_2 + 2\text{Br}$ have been studied for a variety of dissociation energies, $E_{\text{diss}} = 460\text{--}535\text{ kJ mol}^{-1}$ (corresponding to $\lambda = 260\text{--}223\text{ nm}$). The laser induced fluorescence spectrum of nascent CF_2 products was measured for various dissociation energies within this range. Analysis of the spectra yielded the CF_2 vibrational distribution and average rotational energy. The translational energy of CF_2 was measured *via* the Doppler broadening of various fully resolved rovibronic transitions. The most detailed analysis of energy disposal in the CF_2 fragments was carried out at $E_{\text{diss}} = 486\text{ kJ mol}^{-1}$ (or $\lambda = 246\text{ nm}$). At this energy each degree of freedom of CF_2 had an average energy of $E_{\text{vib}} = 0.4 \pm 0.2\text{ kJ mol}^{-1}$, $E_{\text{rot}} = 2.5 \pm 0.5\text{ kJ mol}^{-1}$, and $E_{\text{trans}} = 24 \pm 3\text{ kJ mol}^{-1}$. These CF_2 energies, coupled with the available thermochemical data, allow us to determine unambiguously that CF_2 production must be accompanied by the production of two atomic Br fragments. A photofragment excitation spectrum of CF_2Br_2 , probing for the production of CF_2 fragments, provided a reaction threshold of $460 \pm 3\text{ kJ mol}^{-1}$ (corresponding to $260 \pm 1.5\text{ nm}$). The range of previously published reaction enthalpies varies from 392 to 438 kJ mol^{-1} , all of which are substantially below the observed threshold. Additionally, at $E_{\text{diss}} = 486\text{ kJ mol}^{-1}$, the energy of the CF_2 fragment was 27 kJ mol^{-1} on average, already in excess of the available 26 kJ mol^{-1} , and without considering the kinetic energy of the recoiling Br atoms. We rationalise these data by proposing that the reaction might have a small barrier in the exit channel. The observed threshold corresponds to the top of the barrier (460 kJ mol^{-1}), while the final energy in the fragments is determined by the asymptotic reaction energy ($\sim 424\text{ kJ mol}^{-1}$). Simple dynamical models are presented to show that the proposed mechanism is reasonable. Key future experiments and calculations are identified that would enable a clearer picture of the dynamics of this reaction.

I. Introduction

Scientific interest in halomethanes has been sustained over many decades. Originally, this interest arose due to their many industrial and commercial applications as refrigerants, blowing agents, flame retardants and aerosols. More recently, this interest has continued from the effect these molecules have produced in the atmosphere (particularly chlorofluorocarbons and halons). The well-known ozone depleting cycle is initiated by their photolysis in the stratosphere.^{1,2} A considerable body of work has therefore accumulated on the photolytic reactions of halons, including the molecule investigated here, CF_2Br_2 . Dibromodifluoromethane, or Halon 1202 has been afforded some attention in the popular media of late³ because it is not covered by the Montreal Protocol and its concentration in the atmosphere has been observed to be increasing rapidly over the past few years.⁴

The ultraviolet photodissociation dynamics of CF_2Br_2 have been investigated using a wide variety of methods for almost 40 years. For this halon species, the primary photolysis reac-

tion products have been the subject of some debate over this time. Several pathways have been postulated to be dominant, including:



The reaction enthalpies above are taken from a large compendium of previously published data, and are discussed more fully and referenced in Section IV. Reactions (1)–(3) produce

[†] Current address: Max-Planck-Institut fuer Chemie, Abteilung Luftchemie, Postfach 3060, D-55128 Mainz, Germany.

[‡] Current address: Department of Chemistry, University of Adelaide, Adelaide, South Australia, 5005.

different chemical products, while reactions (3a), (3b) and (3c) each produce CF_2 and two Br atoms, but *via* different mechanisms. Reaction (3a) is the concerted breaking of both C–Br bonds, without the formation of an intermediate. Reaction (3b) is a sequential reaction, where the CF_2Br intermediate is produced. Reaction (3c) likewise involves a CF_2Br intermediate, but the breaking of the second C–Br bond requires a second photon.

The issue of the reaction products of CF_2Br_2 photolysis and the mechanism for this reaction was first discussed in 1960 by Mann and Thrush⁵ who utilised the, then, new technique of flash photolysis to dissociate CF_2Br_2 . Their observation of the CF_2 product (which was supported the following year by Simons and Yarwood⁶) led them to propose reaction (1) as the appropriate pathway.

By 1972, a second reaction pathway had been postulated by Walton.⁷ The dissociation of CF_2Br_2 at 265 nm yielded the detectable products $(\text{CF}_2\text{Br})_2$ and Br_2 . From these results, they concluded that the primary dissociation channel at this wavelength was reaction (2).

In 1978, Sam and Yardley⁸ first used laser photolysis at 248 nm as the means of initiating the photodissociation of CF_2Br_2 . The reaction channel producing CF_2 and Br_2 [eqn. (1)] was supported, although no Br_2 was actually detected. Later, in a similar experiment, Wampler *et al.*⁹ observed the Br_2 molecule in addition to the CF_2 fragments and Br atoms seen by Sam and Yardley. These results led to the conclusion that both reactions 1 and 2 were occurring.

Perhaps the most definitive experiments were carried out by Krajnovich *et al.*¹⁰ in 1984. They also used an excimer laser at 248 nm with a time-of-flight mass spectrometer to detect fragments. They reported CF_2Br^+ and Br^+ ions and concluded that the primary channel at this wavelength is reaction (2). In addition, low concentrations of CF^+ and CF_2^+ were detected. From the flight times of these species it was postulated that they were produced as a result of the secondary photodissociation of the CF_2Br radical [eqn. (3c)], rather than as a result of the spontaneous dissociation of vibrationally hot CF_2Br [eqn. (3b)].

Ultrafast (picosecond) experiments were performed in 1991 by Gosnell *et al.*¹¹ again dissociating CF_2Br_2 at 248 nm. The major products were found to be CF_2Br and Br, but unlike Krajnovich *et al.*, they concluded that the CF_2Br spontaneously dissociated to produce CF_2 and Br [eqn. (3b)]. Evidence for the direct spectroscopic detection of CF_2Br was presented, as well as an interpretation of the spectra based on a slow intramolecular vibrational relaxation (IVR) process. The quantum yield for reaction (3) was estimated to be 20% [the remaining 80% being reaction (2)].

Felder *et al.*¹² used photofragment translational spectroscopy to examine CF_2Br_2 photodissociation dynamics at 193 nm. They concluded that two channels were manifest, the major one being reaction (2), with the CF_2Br fragment formed in unstable states. In addition, reaction (1) was observed (although the Br_2 may have been unstable), which was interpreted as the opening of the molecular channel which could not be accessed in the 248 nm data of Krajnovich.

Multiphoton dissociation at 248 nm was used by van Hoeymissen *et al.*¹³ in 1994 in a study that derived the absorption cross section of CF_2Br . In addition, it was shown that $(30 \pm 10)\%$ of the primary CF_2Br dissociated spontaneously into $\text{CF}_2 + \text{Br}$. This result is in agreement with the work of Gosnell *et al.* described above.

The present work is concerned with a more complete study of the photodissociation dynamics of CF_2Br_2 at a variety of wavelengths between 223 and 260 nm by examination of the nascent energy deposited into the CF_2 fragment. The CF_2 vibrational state distribution and the rotational contour was measured as a function of photolysis wavelength. The translational recoil energy of the CF_2 fragment was estimated by

Dopplerimetry. Finally, the photofragment excitation spectrum of CF_2Br_2 was measured near the threshold for CF_2 production. These data lead to unambiguous determination of the reaction products, the energetic threshold for the reaction, and a discussion of possible reaction mechanisms.

II. Experimental

Dibromodifluoromethane (CF_2Br_2 , 98%, Aldrich) was used throughout with no further purification. A slush bath of ethanol and water maintained the sample at a temperature of approximately -40°C . Helium at a pressure of 2 atm was passed over this sample, and the resultant 2–3% CF_2Br_2 –He mixture was expanded into a vacuum chamber through a pulsed nozzle (Precision Instruments, PV-M3) with a 0.5 mm diameter exit orifice. The free-jet chamber has been fully described previously.¹⁴ The expansion was then crossed approximately 7 mm downstream by either one or two lasers.

For one-laser experiments, the output from a frequency doubled dye laser (Lambda Physik LPD 3001e) pumped by a XeCl excimer laser (Lambda Physik Lextra 200) was used to both dissociate the CF_2Br_2 and probe the nascent CF_2 fragments. This was possible as a result of the coincidental nature of the CF_2Br_2 and CF_2 absorption spectra (see Section III). The laser was scanned continuously from 246 to 262 nm, using C503 dye and a BBO doubling crystal.

Experiments were also conducted in which the pump and probe lasers were independently tunable. The lasers entered the chamber mutually perpendicular to the free jet expansion. Thus, the CF_2 fragments that were probed could only have come from parent molecules in the coldest part of the expansion. The probe laser was the excimer pumped dye laser described above. The photolysis laser was either a Raman shifted Nd:YAG laser (Continuum Surelight I-20) or a frequency doubled (BBO) Nd:YAG pumped dye laser (Continuum Surelight II-10, Lambda Physik Scanmate, C503 dye). The Raman shifted Nd:YAG provided fixed wavelengths within the absorption profile of CF_2Br_2 by selecting various anti-Stokes Raman lines from either the 355 or 266 nm Nd:YAG harmonic, including 266, 246, 238, 223 and 218 nm. The doubled dye laser was used to tune continuously from 246 to 264 nm (the tuning range of C503 dye). The linewidth of the Raman shifted laser was about 2 cm^{-1} . Both doubled dye lasers were approximately 0.3 cm^{-1} linewidth, although this was narrowed by an etalon to $\sim 0.1\text{ cm}^{-1}$ when higher resolution was necessary. The probe laser was timed to arrive approximately 100 ns after the pump beam in order to detect only nascent CF_2 . Nascent CF_2 spectra were measured by fixing the frequency of the pump laser while scanning over various CF_2 transitions. Alternatively, a photofragment excitation (phofex) spectrum could be measured by fixing the probe laser frequency corresponding to a particular CF_2 transition and scanning the pump laser.

In all experiments performed, fluorescence from the nascent CF_2 fragments was imaged using a quartz lens ($f = 50\text{ mm}$) onto the entrance slits of a SPEX Minimate monochromator used to filter scattered laser light. The monochromator bandpass was set at 20 nm. A photomultiplier (EMI 9789QB) detected fluorescence signal through the monochromator, which was subsequently processed by a boxcar integrator (SRS-250), displayed on a Tektronix TDS-320 oscilloscope, and recorded on a personal computer. The timing of the excimer and YAG lasers, nozzle valve and electronics was controlled by a digital delay generator (SRS DG-535).

During the course of each spectrum the power of the scanning laser was monitored and recorded by directing a back reflection from one of the steering prisms onto a cuvette containing Rhodamine 6G dye. Fluorescence from the dye was detected by a fast silicon photodiode, processed by a PAR 162/165 boxcar integrator and sent to the same computer. The

CF₂ fluorescence signal was then corrected for any change in the scanning laser power. The power of the non-scanning laser in a two-laser experiment, was not measured continuously, however, it was monitored before and after scans.

III. Results

A. Absorption spectra of CF₂Br₂ and CF₂

The upper panel in Fig. 1 shows the ultraviolet absorption spectrum of room temperature CF₂Br₂ vapour taken in a Cary-4 UV/VIS spectrometer. The spectrum is featureless with a maximum near 227 nm and absorption that continues to the red beyond 300 nm. The diffuseness and Gaussian band shape are typical of a transition to a directly dissociative electronic state.

The electronic spectrum of the CF₂ molecule, unlike that of its parent, is highly structured. The lowest panel in Fig. 1 shows a low resolution scan of the $\tilde{A}^1B_1 \leftarrow \tilde{X}^1A_1$ electronic transition of jet-cooled CF₂, formed after pyrolysis of CF₂Br₂ in a heated nozzle apparatus as described previously.¹⁵ It clearly shows the strong progression in the ν_2 bending mode originating from the (0,0,0) level in the ground electronic state, along with hot band sequences arising from the (0,1,0) and (0,2,0) levels. Elevated vibrational temperatures precipitated by the hot nozzle conditions caused the hot bands to be more intense in this spectrum than would be detected in a normal room temperature scan. The vibronic origin is located at 268.7 nm¹⁶ with the ν_2 progression extending to higher energy. The maximum in the Franck-Condon intensity distribution lies near 250 nm, corresponding to the (0,5,0) \leftarrow (0,0,0) transition. The absorption spectra of these two species, the parent and fragment in the reaction, are therefore strongly overlapping. This caused some experimental problems in distinguishing two-laser pump-probe signal from one-laser pump-alone or

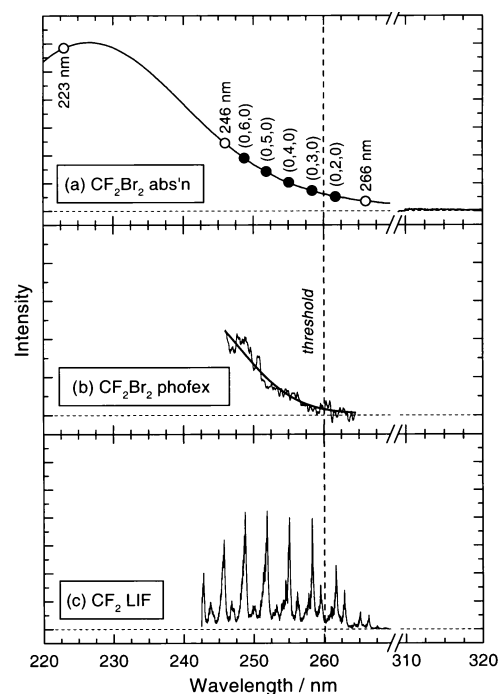


Fig. 1 (a) Room temperature absorption spectrum of CF₂Br₂ vapour. The points indicated on the spectrum represent dissociation wavelengths used in this work, either as one laser (solid circles) or two laser (open circles) experiments. (b) Photofragment excitation spectrum of CF₂Br₂. The signal in the phofex spectrum has fallen to essentially zero by 260 nm, whereas the absorption spectrum continues to almost 300 nm; (c) jet-cooled CF₂ LIF spectrum taken using a pyrolysis nozzle (see text); the CF₂ vibrational assignments in panel (a) refer to the strong peaks in this spectrum.

probe-alone signal. Details of how these problems were dealt with and turned to advantage will be described as appropriate in the following sections.

B. Estimating the threshold for CF₂ production

Establishment of the energy threshold for the production of CF₂ from CF₂Br₂ is an essential ingredient in determining the chemical pathway by which CF₂ is produced, and to understand the dynamics of its production. Three different types of experiments were carried out in an attempt to measure this threshold. In the first set of experiments, a single laser was used to both dissociate CF₂Br₂ and probe CF₂. Fig. 2 shows a series of low resolution, nascent CF₂ spectra, probed *via* different vibronic transitions. In all cases the transitions are $\tilde{A}(0,\nu_2,0) \leftarrow \tilde{X}(0,0,0)$, probing the vibrationless level of the CF₂ product. The dissociation energy varies from approximately 38 200 cm⁻¹ (lower panel) to 40 200 cm⁻¹ (upper panel) throughout these spectra. Since it is a one-laser experiment, the CF₂ wavenumber on the abscissa is also the dissociation wavenumber. The solid symbols in the upper panel of Fig. 1 show the position of the dissociation wavelength in reference to the CF₂Br₂ absorption band. Within any one vibronic band the difference in dissociation energy is only slight (approximately 100 cm⁻¹) and is unlikely to have a significant effect on the qualitative results.

Three observations are particularly noteworthy in the spectra in Fig. 2. Firstly, when the laser is tuned near 38 200 cm⁻¹ (261.5 nm) no CF₂ signal is observed. The (0,2,0)

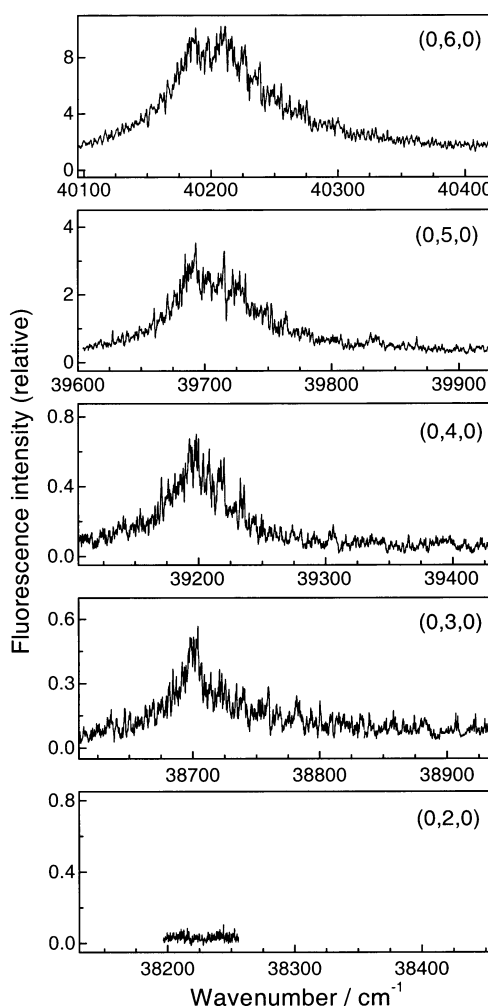


Fig. 2 Nascent CF₂ LIF spectra following dissociation of CF₂Br₂. The same laser is used as both pump and probe. The spectra broaden with higher pump energy, and no CF₂ signal was observed for pump energies below 38 600 cm⁻¹.

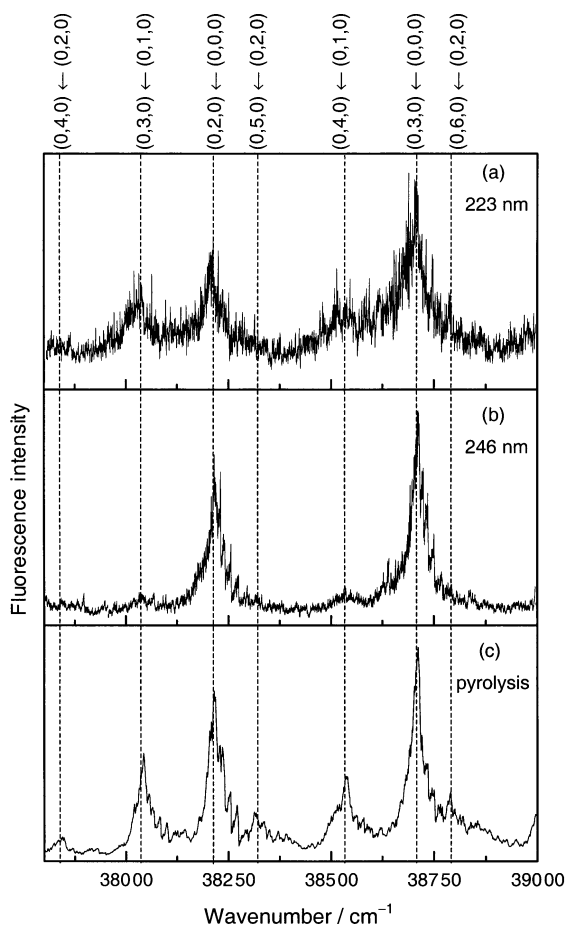


Fig. 3 Low resolution, nascent CF_2 LIF spectra obtained following CF_2Br_2 dissociation at (a) 223 and (b) 246 nm. The spectrum in panel (c) is the same as in Fig. 1(c), using the properties of the pyrolysis nozzle and jet-cooling to enhance vibrational hot-bands. Population in CF_2 ($v_2 = 1$ and 2) is much more significant for the higher energy photolysis energy, though not as much as in the pyrolysis experiment.

$\leftarrow (0,0,0)$ band should lie in this region,¹⁶ [see Fig. 1] centred at $38\,211.7\text{ cm}^{-1}$. At slightly higher energy ($38\,700\text{ cm}^{-1}$ or 258.4 nm) the CF_2 signal is obvious and corresponds to the $(0,3,0) \leftarrow (0,0,0)$ transition. Our detection threshold for CF_2 production from CF_2Br_2 photolysis (which may or may not be the energetic threshold) is therefore located between $38\,200$ and $38\,700\text{ cm}^{-1}$ (or 258.4 and 261.8 nm).

The second observation from Fig. 2 is that the CF_2 rotational contour broadens as the dissociation energy is increased. The width of the contour is an indication of the amount of CF_2 rotational excitation produced in the reaction, which increases with increasing dissociation energy (see also section III. C).

The third observation concerns the intensity of each spectrum, indicated by the scale on the ordinate. The intensity of the CF_2 LIF spectrum increases markedly from lower to higher energy. The reasons are twofold: the absorption coefficient of the CF_2Br_2 parent is increasing rapidly over this range [see Fig 1(a)], and also the CF_2 Franck–Condon factors increase monotonically from the lowest spectrum to a peak at the $(0,5,0) \leftarrow (0,0,0)$ transition¹⁷ [see Fig. 1(c)].

The first and third observations above are linked because the intensity of the CF_2 fluorescence signal drops off with decreasing energy due to both the CF_2Br_2 and CF_2 absorption strengths. It is reasonable to question whether the lack of signal near 261.5 nm is due to an energetic constraint or simply to the combined reduction in CF_2Br_2 and CF_2 absorption coefficients and our subsequent ability to detect the fragments. To examine this question information may be extracted from the signal-to-noise (S/N) ratios in the

spectra. The spectrum observed after pumping/probing the $(0,3,0) \leftarrow (0,0,0)$ vibrational band exhibits $S/N \approx 13$. The absorption strength of CF_2Br_2 drops by a factor of 1.4 between 258.4 and 261.7 nm (using the room temperature spectrum as an estimate). The CF_2 Franck–Condon factor for the $\tilde{A}(0,2,0) \leftarrow \tilde{X}(0,0,0)$ transition (at 261.7 nm) drops by 2.4 in comparison with the $\tilde{A}(0,3,0) \leftarrow \tilde{X}(0,0,0)$ transition.¹⁷ Therefore a CF_2 spectrum with $S/N \approx 4$ would be expected, (before accounting for the increase in signal that would be created by the smaller rotational partition function for CF_2 at this lower energy). Consequently, it seems that if CF_2Br_2 is absorbing light and dissociating to produce CF_2 then the spectrum should have been observed.

Additional evidence is provided by the spectra in Fig. 2, which show that the rotational envelopes become narrower as the dissociating/probing energy is decreased. The decreasing width of the rotational contours indicate that the rotational energy in the CF_2 fragment is also decreasing, due to the lower amount of energy imparted in the original photo-dissociation event. The fact that this contraction is quite marked from 255 to 260 nm suggests that the reaction threshold for the formation of CF_2 is near.

A series of two-laser experiments were performed to try and isolate the effects of diminishing CF_2Br_2 and CF_2 absorption strength with decreasing energy. In these experiments the probe laser was kept fixed at the CF_2 origin transition at 268.7 nm (well below the one laser detection threshold) while the photolysis laser was scanned from 246 to 265 nm (the range of C503 dye). The ensuing photofragment excitation (phofex) spectrum, corrected for the changing laser power over this range is shown in Fig. 1(b). The “structure” in the phofex spectrum is not reproducible but is an indicator of the underlying noise in the spectrum. A Gaussian fit has been overlaid as a guide for comparison of this spectrum with the absorption spectrum above it. Near 260 nm , where the room temperature absorption spectrum is still registering a significant level of absorption, the signal in the phofex spectrum has reached essentially zero.

Finally, a two-laser experiment was performed, attempting to dissociate CF_2Br_2 at 266 nm , where more than two orders of magnitude additional laser power was available to circumvent the weaker absorption strength. The probe laser was set at 261.7 nm , *i.e.* for detection *via* the $\tilde{A}(0,2,0) \leftarrow \tilde{X}(0,0,0)$ transition. However, the large increase in photolysis power was ineffective as no CF_2 signal could be observed at this wavelength.

The conclusion from the evidence above is that for energies below $38\,450 \pm 250\text{ cm}^{-1}$ ($\lambda > 260 \pm 1.5\text{ nm}$) the excited CF_2Br_2 molecules dissociate to form CF_2Br and a Br atom. At higher photolysis energies the molecules are sufficiently excited to form CF_2 and two atomic Br fragments.

C. CF_2 product state distributions

The one-laser experiments sketch out an overview of the CF_2Br_2 dissociation mechanism that includes a threshold near $38\,450\text{ cm}^{-1}$ and increasing rotational excitation of the CF_2 fragment as the energy above this threshold is increased. However, these experiments are not ideal for measuring the details of the energy deposited in the CF_2 fragment because the available energy is changing throughout the spectrum, as is the absorption strength of the parent. Therefore, the experiments from which energy distributions are obtained are all two-laser experiments with a fixed photolysis frequency. All two-laser experiments were designed so that any ‘pump alone’ or ‘probe alone’ signal had been minimised or eliminated. This included temporal separation, the use of monochromators and reduction in laser intensity. Vibrational distributions were obtained from a variety of photolysis wavelengths in the range 223 – 259 nm . Rotational temperatures were esti-

mated from spectral contour fitting over the range $\lambda_{\text{diss}} = 246\text{--}259$ nm. Sub-Doppler line shapes were measured for several single rovibronic transitions for photolysis at 246 nm.

Vibrational distribution. Vibrational distributions were measured for a variety of wavelengths between 258 and 250 nm, and then two further fixed wavelengths, 246 and 223 nm, which are the 3rd and 4th anti-Stokes Raman shifted wavelengths from the 355 nm Nd : YAG harmonic. An overview of the CF_2 spectra produced in the 246 and 223 nm dissociation of CF_2Br_2 , showing the “hot” vibrational structure, is shown in Fig. 3. Part of the strong progression in the ν_2 bending mode is shown, namely $(0, \nu_2, 0) \leftarrow (0, 0, 0)$ for $\nu_2 = 2$, and 3. Reproduced below these spectra is the CF_2 spectrum produced in a pyrolysis nozzle followed by free jet expansion. The combination of the properties of the pyrolysis nozzle and differing rates of cooling in the free jet for the different degrees of freedom accentuates the vibrational hot bands. The most prominent of these progressions originates from the $(0, 1, 0)$ vibrational state, and is labelled in the figure. Comparison of the spectra in Fig. 3(a) and 3(b) with that in Fig. 3(c) immediately highlights the important feature of the former, *viz.*, there is very little vibrational hot band activity in the nascent spectrum.

The vibrational energy distributions were calculated from these spectra using the integrated intensities of the transitions, $(0, 2, 0) \leftarrow (0, 0, 0)$, $(0, 3, 0) \leftarrow (0, 0, 0)$, $(0, 3, 0) \leftarrow (0, 1, 0)$, $(0, 4, 0) \leftarrow (0, 1, 0)$ and $(0, 4, 0) \leftarrow (0, 2, 0)$. The intensities were scaled by their respective Franck–Condon factors.¹⁷ The sum of the population in the states was then normalised. These vibrational distributions are shown in Fig. 4. The circles represent the normalised populations. The line fitted to the data represents the expected vibrational distribution in CF_2 for temperatures of 150, 325 and 650 K. The average vibrational energy of the CF_2 fragments was calculated from this distribution by directly summing the energy of each of the states scaled by its normalised population. The average vibrational energies, E_{vib} , calculated in this manner are shown in Table 1.

2. Rotational energy. The rotational contour of $(0, 5, 0) \leftarrow (0, 0, 0)$ band of CF_2 following 246 nm dissociation is shown in Fig. 5. In comparison, the same spectrum, using the same laser, was measured for thermalised (300 K) CF_2 and is shown beneath. The contour of the nascent spectrum is clearly narrower than the 300 K spectrum. In the nascent spectrum the 1R_K band heads (labelled in the figure) decrease sharply with increasing K , so much so that by $K = 5$ they are no longer clearly distinguishable from the surrounding rotational structure. By comparison, the band heads in the thermal spectrum

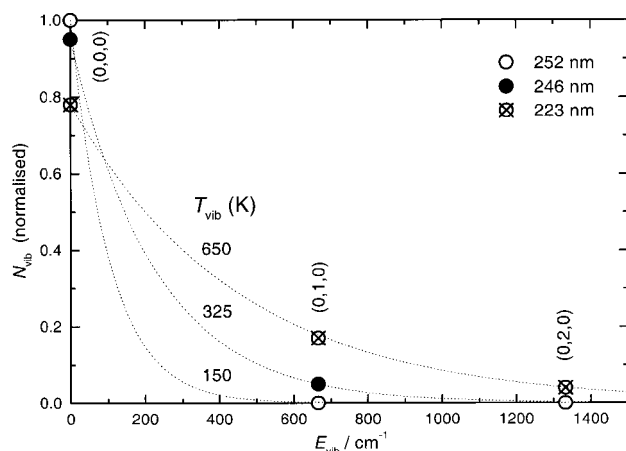


Fig. 4 CF_2 vibrational state population distributions for three photolysis wavelengths. Boltzmann distributions corresponding to temperatures of 150, 325 and 650 K are indicated for comparison.

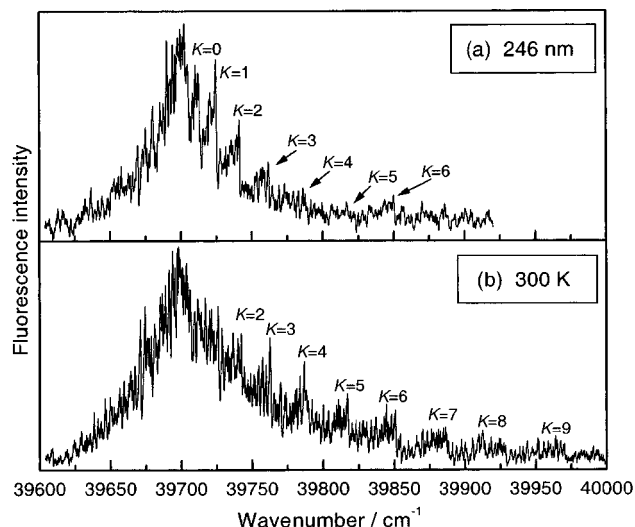


Fig. 5 Medium resolution scan of the CF_2 $(0, 5, 0) \leftarrow (0, 0, 0)$ transition. (a) Nascent CF_2 following dissociation of CF_2Br_2 at 246 nm; (b) thermal (300 K) CF_2 . The nascent spectrum has a narrower contour, indicating less rotational energy than thermal CF_2 .

are identifiable even for $K = 9$. This indicates that the rotational energy of the nascent fragments is less than that available at room temperature. These contours were simulated at various temperatures using the ASYROT asymmetric rotor program of Birss and Ramsay¹⁸ and rotational constants of Mathews.^{16,19} The thermal spectrum was modelled well, but the nascent spectrum less so. Although it is possible to model the decrease in 1R_K band intensity, to do so would require a rotational temperature substantially colder than 100 K. Such low temperatures, however, have very little surrounding rotational structure, whereas the nascent spectrum is rich in rotational structure. It is therefore impossible to fit exactly a single temperature to the nascent spectrum. A simulation at 200 K represented the best compromise. At this temperature the band head intensity decreases fairly rapidly, yet the rotational complexity is preserved. A temperature of 200 K corresponds to a rotational energy $(3/2kT)$ of 210 cm^{-1} or 2.5 kJ mol^{-1} .

3. Translational energy. Repeated high resolution etalon scans were taken of nine non-overlapping rotational transitions for photolysis at 246 nm. The transitions chosen were, in the 1R_3 branch; ($J'' = 9, 10$ and 11), in the 1R_4 branch; ($J'' = 8, 10, 11, 16, 22$) and ${}^1Q_4(14)$. Fig. 6 shows the Doppler profiles of the ${}^1R_4(10)$ and ${}^1R_4(11)$ peaks, with a small unassigned transition between them. The line width of the laser, estimated to have a full width at half maximum (fwhm) of 0.10

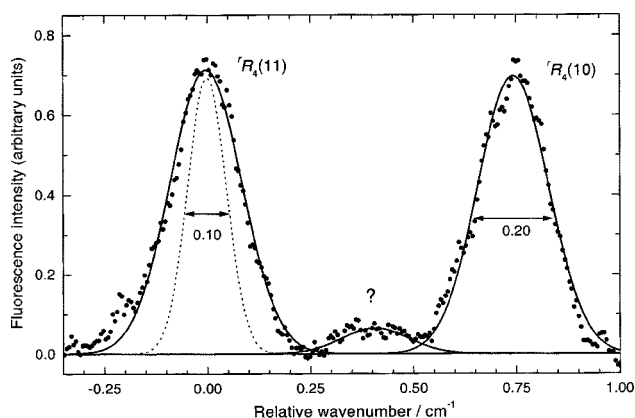


Fig. 6 High resolution scan of a small region of the nascent spectrum in Fig. 5. The laser line width is 0.10 cm^{-1} and is indicated by a dotted line. Solid lines through the three peaks are Gaussian functions with a fwhm of 0.20 cm^{-1} .

cm^{-1} is shown as a dotted line. It is apparent from this figure that the Doppler width of the recoiling CF_2 fragment is only slightly broader than the laser line width indicating that the recoiling fragments do not possess a large velocity.

To estimate the average translational energy, we fit each peak to a Gaussian function (shown in the figure) and extracted the fwhm. The fitting routine allowed the peak position, height and width to vary without constraint for the two larger peaks. In both cases, a fwhm of $0.204 \pm 0.010 \text{ cm}^{-1}$ resulted. For the Gaussian fit to the central peak the width was held at this value and only the position and height allowed to vary. To compensate for the broadening of the transition due to the laser line width, the fwhm of the peak was deconvolved with the fwhm of the laser. The deconvolved peak width of the $K = 4$ data is $0.173 \pm 0.010 \text{ cm}^{-1}$. This corresponds to a translational temperature of $1950 \pm 200 \text{ K}$, or an average translational energy of $E_{\text{trans}} = 2030 \pm 200 \text{ cm}^{-1}$ or $24.3 \pm 3.0 \text{ kJ mol}^{-1}$.

At lower photolysis energies the signal strength dropped off significantly, and line widths approached the laser line width. At much higher photolysis energies rotational congestion and broader Doppler widths prevented measurement of clean, single rovibronic transitions. Consequently, we have only been able to estimate the nascent CF_2 kinetic energy for the single photolysis wavelength reported above, *i.e.* $\lambda = 246 \text{ nm}$.

D. Summary of data

In the experiments above we have determined the threshold for production of CF_2 fragments from the photolysis of CF_2Br_2 to be at $260 \pm 1.5 \text{ nm}$, corresponding to a threshold energy of $460 \pm 3 \text{ kJ mol}^{-1}$. The nascent energy deposited into the vibrational, rotational and translation degrees of freedom of the CF_2 fragment has been measured for a variety of photolysis wavelengths, most completely for $\lambda_{\text{diss}} = 246 \text{ nm}$. Most of the energy released to the CF_2 fragment in this reaction is dissipated into translational motion, with a smaller amount into rotation and an almost negligible amount into vibration. The nascent vibrational energy released into CF_2 following dissociation at 252.5 and 223 nm was also measured. The CF_2 vibrational energy was shown to increase with increasing photolysis energy, although remaining fairly small throughout. The average energy in each degree of freedom is reported in Table 1 as a function of photolysis wavelength.

IV. Discussion

Many workers have examined the photodissociation of CF_2Br_2 at wavelengths similar to those employed here. Excitation into the first band system of CF_2Br_2 corresponds to a $B_1 \leftarrow A_1$ transition.^{10,20} Although early workers observed or inferred Br_2 as a product,^{5–8} later work appears to support Br_2 not being a primary product.^{10,21} The dominant channel at 248 nm is the simple C–Br bond cleavage yielding the CF_2Br radical and atomic Br (either $^2P_{3/2}$ or $^2P_{1/2}$). The tran-

sient absorption spectrum of CF_2Br has been reported by several groups.^{11,13,22,23} The spectrum appears to evolve with time in the first few picoseconds of formation of CF_2Br . This suggests that the fragment is born with a non-statistical distribution of vibrational energy, which then randomises over this timescale.¹¹

The formation of CF_2 has been somewhat more controversial. Observations have been plentiful, especially in infrared multiphoton dissociation of CF_2Br_2 ,^{24–27} the mechanism for its formation not so clear. Early workers postulated Br_2 formation, which has been subsequently discounted. Krajnovich *et al.* suggested that it is only formed when primary CF_2Br fragments absorb a second photon. The weight of most recent opinion is that CF_2 may be produced as a primary product at 248 nm with quantum yields varying from 1–30%.^{11,13,21,23}

The quantum yield of Br atom production has been measured as 1.01 ± 0.15 at 248 nm and 1.63 ± 0.19 at 222 nm. These values are consistent with 1% of hot CF_2Br having sufficient energy to spontaneously break the C–Br bond at 248 nm, rising to 63% at 222 nm. The electronic state of the Br fragment is not well-known. Talukdar *et al.* report the observation of both ground ($^2P_{3/2}$) and excited ($^2P_{1/2}$) spin-orbit states, however, the relative abundance of each was not reported.²¹

In the experiment described above we have measured the nascent internal and translational energy of CF_2 . The threshold to CF_2 production has also been measured. Below we discuss how the observed energetics relate to the picture of CF_2Br_2 chemistry that has been sketched out above.

A. The appropriate reaction for CF_2 formation

There are two different reaction pathways that could lead to the formation of CF_2 from CF_2Br_2 at the wavelengths used in this work: (i) formation of CF_2 and molecular bromine [reaction (1)]; (ii) formation of CF_2 and two bromine atoms [reactions (3a, b, c)]. Heats of formation and hence reaction enthalpies are not particularly well-known for the species and reactions involved. Table 2 summarises the range of values in the recent literature, as well as the values that we have used here. The heats of formation of CF_2 , Br and Br_2 are reasonably secure. However CF_2Br_2 is known with only moderate accuracy, and CF_2Br is poorly known. Even so, the values in Table 2, coupled with the energy deposited in the CF_2 fragment enable an unambiguous determination of the appropriate chemical pathway in this instance.

Firstly, we can conclude that CF_2 is produced after absorption of only one photon. We measured the dependence of CF_2 signal on photolysis laser power and observed a linear dependence (not shown).²⁰ However, as previous workers have discussed,^{10,11,13} this alone is not a definitive result. If two photons were absorbed then there would be an extra 486 kJ mol^{-1} (the photon energy) to be disposed of in the fragment degrees of freedom. The total CF_2 energy is only 27 kJ mol^{-1} , leaving about 480 kJ mol^{-1} to be deposited in the trans-

Table 1 Summary of average energy in each degree of freedom of CF_2 for three different photolysis wavelengths

$\lambda_{\text{diss}}/\text{nm}$	$E_{\text{excess}}/\text{kJ mol}^{-1a}$	CF_2 average energy/ kJ mol^{-1} (% E_{excess})			
		Vibration	Rotation	Translation	Total
252.5	14 ± 3	0 (0%)	1.3 ± 0.5 (9 ± 4%)	—	—
246	26 ± 3	0.4 ± 0.1 (1.5%)	2.5 ± 0.5 (10 ± 2%)	24.3 ± 3.0^b (94 ± 8%)	27.2 ± 2.5 (106 ± 10%)
223	76 ± 3	3.7 ± 0.6 (5%)	—	—	—

^a Relative to CF_2 detection threshold at $460 \pm 3 \text{ kJ mol}^{-1}$. ^b Determined specifically for $K_a = 3$ or 4, $J = 8–22$. The average translational energy for all CF_2 states is likely to be slightly lower than this.

Table 2 Enthalpies of formation and reaction used in this work

Species or reaction	$\Delta_f H_{298}^0$ or $\Delta_r H_{298}^0$ range quoted/ kJ mol ⁻¹	Refs.	$\Delta_f H_{298}^0$ or $\Delta_r H_{298}^0$ preferred value/ kJ mol ⁻¹	Ref.
CF ₂ Br ₂ (g)	-362 to -382	12, 20	-382 ± 11	20
CF ₂ Br (g)	-219 to -225	10, 12, 20	-220 ± 8	20
CF ₂ (g)	-172 to -194	10, 12, 20, 28	-182 ± 5	28
Br (g)	112 to 118	10, 12, 29	111.87 ± 0.12	29
Br ₂ (g)	31	29	30.91 ± 0.11	29
CF ₂ Br ₂ → CF ₂ + 2 Br	392 to 438	12, 21, 23, 24	424 ^a	
CF ₂ Br ₂ → CF ₂ + Br ₂	213 to 225	9, 12, 21, 22, 23	231 ^a	
CF ₂ Br ₂ → CF ₂ Br + Br	248 to 276	7, 10, 12, 13, 21, 22, 23, 24	274 ^a	
CF ₂ Br → CF ₂ + Br	146 to 160	10, 12, 13	150 ^a	
Br ₂ → 2 Br	193		193 ^a	

^a Calculated from preferred heats of reaction. In the case of CF₂Br₂ → CF₂ + Br₂ this results in the preferred value lying slightly outside the range of previously quoted values.

lational energy of the two recoiling bromine atoms. The translational energy of the CF₂ is only 24 kJ mol⁻¹ and therefore it is difficult to construct a plausible mechanism where the two heavier atoms receive vastly more translational energy than the lighter CF₂ species. Only a contrived mechanism in which the two bonds break in a concerted manner with the bromine atoms recoiling directly away from each other could produce such a result. Such a result also makes the CF₂ appearance threshold of 460 kJ mol⁻¹ difficult to rationalise in any way. Therefore, we reject this scenario as highly improbable.

The formation of molecular bromine can also be discounted at these wavelengths. At $\lambda_{\text{diss}} = 246$ nm, almost half of the 486 kJ mol⁻¹ photon energy is required to overcome the reaction endothermicity (231 kJ mol⁻¹). The remainder (255 kJ mol⁻¹) is available to be distributed amongst the fragment degrees of freedom. Table 1 shows that the total energy of the CF₂ has been estimated to be 27 kJ mol⁻¹, 24 of which is translational energy. Since linear momentum must be conserved, the sibling Br₂ fragment must possess 7.5 kJ mol⁻¹ of translational energy. By difference, therefore, the average internal energy of the Br₂ molecule formed must be about 220 kJ mol⁻¹. This amount is in excess of the energy required to dissociate Br₂ (192 kJ mol⁻¹), in which case bromine atoms and not molecules would be formed. (Note that we are not discounting a potential energy surface that leads to Br₂, but where the Br₂ is too energetic to be stable. At this stage we make no claim about the potential energy surfaces involved in the reaction mechanism, but simply that the ultimate chemical products associated with CF₂ formation must be two atomic Br fragments.)

The only remaining pathway is production of CF₂ and two bromine atoms. Using a single 246 nm photon, this leaves about 62 kJ mol⁻¹ to be divided between the three fragments according to the values in Table 2. About 27 kJ mol⁻¹ are accounted for in the CF₂ fragment leaving 35 kJ mol⁻¹ in translational energy of the two bromine atoms. This amount of translational energy is easily justified. A simple kinematic calculation, starting with a tetrahedral CF₂Br₂ structure, allowing the two (ground state) bromine atoms to be released simultaneously to create a CF₂ fragment with 24 kJ mol⁻¹ of kinetic energy and conserving linear momentum, requires that the energy of the bromine atoms be 11.5 kJ mol⁻¹ each. This is sufficiently close to the 35 kJ mol⁻¹ required (fortuitously close for the assumptions made), and provides confidence that the energy balance for the CF₂ + 2 Br channel is reasonable.

B. Energetic threshold for the production of CF₂

The heats of formation used above proved to be sufficiently accurate to determine that CF₂ production must be accompa-

nied by two Br atoms because the energy differences between the chemical channels were large. However, the uncertainty in the published heats of formation in Table 2 reveal an uncertainty of up to 46 kJ mol⁻¹ in the energy threshold. For discussion of the mechanism of CF₂ production a more accurate threshold is desirable.

The most reliable values in Table 2 seem to indicate a value of $\Delta_r H_{298}^0 \approx 424$ kJ mol⁻¹ for breaking both C–Br bonds in CF₂Br₂. We presented evidence above for a threshold of 460 kJ mol⁻¹. The evidence included two different types of threshold measurements, and an unsuccessful attempt to measure CF₂ signal with a high intensity 266 nm source. Thermochemical values for bromine-containing compounds are not very reliable, yet this discrepancy seems significant. An appearance threshold, of course, need not be associated with a thermochemical threshold. There are several scenarios that that would give rise to an appearance threshold lying above the thermochemical threshold: (i) If one or both of the Br atoms were produced in an excited electronic state, then the appearance threshold for CF₂ would be higher by this amount. There has been one previous measurement of the Br spin-orbit state populations, which indicated that both ground state Br(²Π_{3/2}) and excited state Br*(²Π_{1/2}) are produced, although the relative population of each was not reported.²¹ The higher spin-orbit component lies 44.10 kJ mol⁻¹ above the ground state which, using the values in Table 2, would place the threshold for production of CF₂ + Br(²Π_{3/2}) + Br(²Π_{1/2}) at 468 kJ mol⁻¹. While this places the threshold in closer agreement with the observed threshold, it does not solve the problem of the excess energy in the fragments. At a dissociation energy of 486 kJ mol⁻¹, there would only be ≈ 18 kJ mol⁻¹ available for CF₂, Br and Br*. Yet 27 kJ mol⁻¹ is found in CF₂ alone, and another ~ 23 kJ mol⁻¹ is likely to be found in translational energy of the Br fragments (based on conservation of momentum). Therefore, although a pathway in which one of the Br fragments is electronically excited helps to rationalize the appearance threshold, it fails to account for the energy disposal. Therefore, we believe that two ground state Br(²Π_{3/2}) atoms are the most likely siblings to the CF₂ fragment. We note that this is not in disagreement with the observation by Talukdar *et al.*, who observed both spin-orbit states at a similar energy to that used here. Several groups^{10,11,13,21,23} have reported that, at wavelengths around 248 nm, the largest fraction (probably $\sim 80\%$) of CF₂Br₂ molecules decompose to form CF₂Br and Br, where the CF₂Br is stable with respect to further spontaneous dissociation. Therefore any experiment that probes for Br production at this wavelength must observe Br from both the CF₂Br + Br channel, and the CF₂ + 2Br channel. At these energies, the CF₂Br + Br channel has ample excess energy (212 kJ mol⁻¹ according to Table 2) to produce

Br*. (ii) When the reaction energy lies very close to the threshold the rate of reaction slows considerably (an effect modelled well by transition state theory³⁰). In these experiments, we probe for products 100 ns after the photolysis event. This time is sufficiently short to prevent collisions in the beam, however, it is a long time scale for intramolecular vibrational redistribution (IVR). Indeed, in CF₂Br the time scale for complete IVR at these energies has been measured to be in the order of 6 ps.¹¹ Also, the appearance threshold is ~ 35 kJ mol⁻¹ above the thermochemical threshold. In molecules of this size, this is too far above the threshold for kinetic constraints to be observed on a nanosecond time scale. Therefore we reject a kinetic constraint as being responsible for the observed threshold in this case. (iii) A barrier in the exit channel would also provide an appearance threshold that lies above the thermochemical value. Such a barrier is shown schematically in Fig. 7. In the figure the asymptotic product energy is set at the thermochemical value, which is consistent with the average energy found in the CF₂ fragment. The top of the barrier is placed at the appearance threshold, which provides an exit channel barrier in the order of 35 kJ mol⁻¹. In the next section we explore possible origins of such a barrier.

C. The barrier ?

There has been no study, either experimental or theoretical, on the reaction of CF₂Br \rightarrow CF₂ + Br, nor the reverse reaction. There is also no experimental data, to our knowledge, on the dissociation dynamics of any halogenated methyl radical to compare with CF₂Br. Therefore, we consider the plausibility of a barrier, and situations where one might arise only in the broadest terms.

There are at least two ways by which a barrier might arise in this system. The ground state of the CF₂Br radical is a doublet with the unpaired electron occupying a σ -like orbital. If the C–Br bond is stretched diabatically, then the resultant products will be a Br atom and a CF₂ molecule with two unpaired electrons (a biradical) as shown in Fig. 8 by following the dashed curve. The ground state of CF₂, however, is a carbene configuration in which the two non-bonding electrons of the carbon occupy the same, in-plane, sp₂-like orbital. Therefore, the adiabatic surface must involve a crossing of the two diabatic surfaces which, when they interact, will form two adiabatic surfaces such as sketched in Fig. 8. Such an avoided crossing commonly leads to the formation of a barrier in the reaction potential energy surface. For example, a similar system is the dissociation of CBrF₃ in the excited electronic state.^{31,32} The diabatic surface for breaking the C–Br bond leads to excited state CF. A similar curve crossing in this

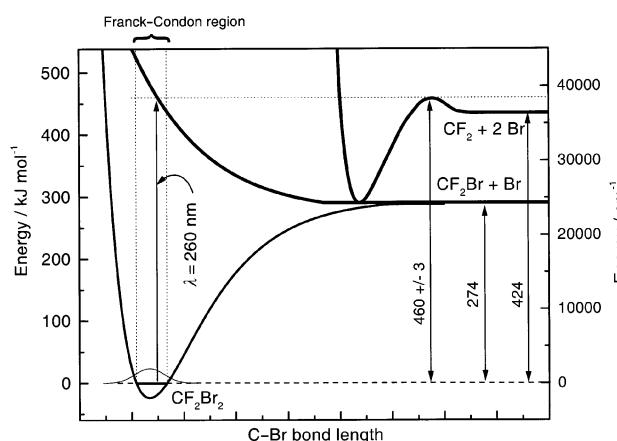


Fig. 7 Schematic of the potential energy surface leading to CF₂Br + Br and CF₂ + 2 Br. Best estimates of the thermochemical enthalpies, based on Table 2 are shown. The hypothesized barrier in the CF₂Br \rightarrow CF₂ + Br channel is indicated.

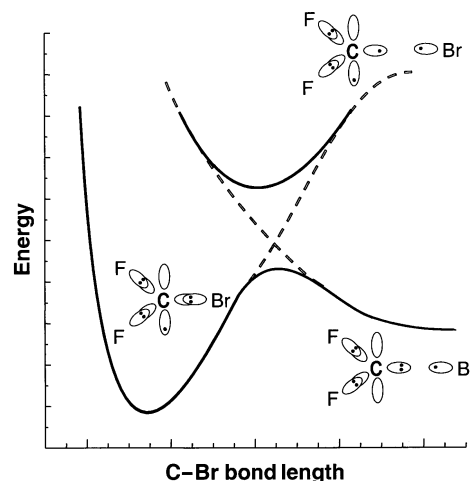


Fig. 8 Picture of the electronic states and electron orbital occupancies of CF₂Br, CF₂ and Br showing how a barrier might eventuate from the interaction of two diabatic surfaces.

system leads to an exit channel barrier of ~ 20 kJ mol⁻¹ en route to production of ground state CF and Br. Of course, whether a barrier is actually formed depends on how strong the interaction is. A very strong interaction may yield a surface that remains below the asymptotic energy of the products and hence a “barrier” is not formed.

Another source of a barrier in the present reaction might arise from the two spin-orbit states of the Br atom, which are separated by 44 kJ mol⁻¹. A similar argument to that presented above would apply for the two states of Br, rather than two CF₂ states. This time the spin-orbit interaction would couple the two surfaces, probably at quite long range. A barrier might again result, depending on the range and strength of the coupling.

The message from the general discussion above is that there are reasonable mechanisms by which a barrier might arise in the dissociation of CF₂Br. Good, high level calculations on this reaction might assist in supporting or refuting the presence of the hypothesized barrier. Such calculations will not be straightforward as they involve open-shell species, heavy atoms, and must include spin-orbit coupling.

More experimental evidence might also elucidate the presence of a barrier. In particular, the detailed rotational distribution of the CF₂ fragment could be quite sensitive to the presence of a barrier, depending on the transition state structure, and the height of the barrier. If the reaction turns out not to have a barrier, then the CF₂ rotational distribution will probably be characterised reasonably by phase space theory or another statistical model. If a barrier exists, then the rotational distribution might be non-statistical and reflect the nature of the barrier. Experimentally, this requires resolving and measuring the hundreds of CF₂ rovibronic transitions. Fig. 5 indicates the complexity of the spectrum, but the resolution shown in Fig. 6 demonstrates that it is feasible.

V. Conclusions and future work

In the present work we have explored the photolysis of CF₂Br₂ at wavelengths between 260 and 223 nm, concentrating mostly at 246 nm. The CF₂ fragment was probed by LIF and the nascent energy in vibration, rotation and translation measured. CF₂ is born vibrationally and rotationally cold (0.4 and 2.5 kJ mol⁻¹ respectively at 246 nm), but with substantially more translational energy (24 kJ mol⁻¹). A threshold for CF₂ production was found at 260 ± 1.5 nm, which corresponds to an energy threshold of 460 ± 3 kJ mol⁻¹. This threshold seems inconsistent with the available, but insecure, thermochemical data, which indicate that the energetic thresh-

old should be closer to $424 \pm 20 \text{ kJ mol}^{-1}$. Analysis of the energy distribution in the CF_2 fragment leads to the unambiguous conclusion that the CF_2 fragment must be formed in concert with two Br atoms. The analysis also suggests that both Br atoms are in their ground $^2\Pi_{3/2}$ state. Comparison with previous experiments, coupled with the analysis of the energy balance suggests that the reaction is a two step process, forming $\text{CF}_2\text{Br} + \text{Br}$ in the first instance, with at least some of the CF_2Br having sufficient energy to produce $\text{CF}_2 + \text{Br}$ spontaneously. We hypothesize that this second step proceeds over a barrier, perhaps about 35 kJ mol^{-1} from the exit channel, to account for the threshold discrepancy.

These conclusions indicate a need for further work. Firstly, high quality *ab initio* calculations should reveal whether the hypothesized barrier is reasonable, although with 2 Br atoms in the system, open shell species and spin-orbit coupling, this will not be a straightforward exercise. Secondly, more detailed experiments, resolving the full J , K rotational distribution might indicate whether a barrier is present. These experiments are likewise non-trivial.

Acknowledgements

The authors thank the Joint Laser Facility (funded by the Australian Research Council) for the loan of a laser used in these experiments. We also thank Dr George Bacskay for continuous discussion about this system, in particular regarding the presence of a barrier. MRC is grateful for an APA post-graduate scholarship.

References

- M. J. Molina and F. S. Rowland, *Nature*, 1974, **249**, 810.
- B. J. Finlayson-Pitts and J. N. Pitts, Jr., *Atmospheric Chemistry: Fundamentals and Experimental Techniques*, Wiley, NY, 1986.
- New Scientist*, 12-September-1998, p. 12; *Sydney Morning Herald*, 31-August-1998, p. 4.
- P. J. Fraser, D. E. Oram, C. E. Reeves, S. A. Penkett and A. McCulloch, *J. Geophys. Res.*, 1999, **104**, 15985.
- D. E. Mann and B. A. Thrush, *J. Chem. Phys.*, 1960, **33**, 1732.
- J. P. Simons and A. J. Yarwood, *Trans. Faraday Soc.*, 1961, **57**, 2167.
- J. C. Walton, *J. Chem. Soc., Faraday Trans.*, 1972, **68**, 1559.
- C. L. Sam and J. T. Yardley, *Chem. Phys. Lett.*, 1979, **61**, 509.
- F. B. Wampler, J. J. Tiee, W. W. Rice and R. C. Oldenberg, *J. Chem. Phys.*, 1979, **71**, 3926.
- D. Krajnovich, Z. Zhang, L. Butler and Y. T. Lee, *J. Phys. Chem.*, 1984, **88**, 4561.
- T. R. Gosnell, A. J. Taylor and J. L. Lyman, *J. Chem. Phys.*, 1991, **94**, 5949.
- P. Felder, X. Yang, G. Baum and J. R. Huber, *Israel J. Chem.*, 1993, **43**, 33.
- J. van Hoeymissen, W. Uten and J. Peeters, *Chem. Phys. Lett.*, 1994, **226**, 159.
- A. C. Terentis, M. Stone and S. H. Kable, *J. Phys. Chem.*, 1994, **98**, 10802.
- M. R. Cameron, S. H. Kable and G. B. Bacskay, *J. Chem. Phys.*, 1995, **103**, 4476.
- C. W. Mathews, *Can. J. Phys.*, 1967, **45**, 2355.
- D. S. King, P. K. Schenck and J. C. Stephenson, *J. Mol. Spectrosc.*, 1979, **78**, 1.
- F. W. Birss and D. A. Ramsey, *Comput. Phys. Commun.*, 1984, **38**, 83.
- C. W. Mathews, *National Research Council, Depository of Unpublished Data*, National Science Library, Ottawa, Canada K1A 0S2, 1967.
- M. R. Cameron, PhD Thesis, University of Sydney, 1998.
- R. K. Talukdar, G. L. Vaghiani and A. R. Ravishankara, *J. Chem. Phys.*, 1992, **96**, 8194.
- R. K. Vatsa, A. Kumar, P. D. Naik, K. V. S. Rama Rao and J. P. Mittal, *Chem. Phys. Lett.*, 1993, **207**, 75.
- R. K. Vatsa, A. Kumar, P. D. Naik, K. V. S. Rama Rao and J. P. Mittal, *Bull. Chem. Soc. Jpn.*, 1995, **68**, 2817.
- B. Abel, H. Hippler, N. Lange, J. Schuppe and J. Troe, *J. Chem. Phys.*, 1994, **101**, 9681.
- R. J. S. Morrison, R. F. Loring, R. L. Farley and E. R. Grant, *J. Chem. Phys.*, 1981, **75**, 148.
- M. E. Jacox, *Chem. Phys. Lett.*, 1978, **53**, 192.
- D. S. King and J. C. Stephenson, *Chem. Phys. Lett.*, 1977, **51**, 48.
- M. W. Chase, Jr., *NIST-JANAF Thermochemical Tables, Fourth Edition*, *J. Phys. Chem. Ref. Data*, Monograph 9, 1998, pp. 1–1951.
- J. D. Cox, D. D. Wagman and V. A. Medvedev, *CODATA Key Values for Thermodynamics*, Hemisphere Publishing Corp., New York, 1984, p. 1.
- See, for example, R. G. Gilbert and S. C. Smith, *Theory of Unimolecular and Recombination Reactions*, Blackwell, Oxford, 1990.
- P. T. Knepp, C. K. Scalley, G. B. Bacskay and S. H. Kable, *J. Chem. Phys.*, 1998, **109**, 2220.
- P. T. Knepp and S. H. Kable, *J. Chem. Phys.*, 1999, **110**, 11789.